Bull. Min. Res. Exp. (2026) 179: 124-137

Bulletin of the Mineral Research and Exploration

http://bulletin.mta.gov.tr

An alternative approach to estimate the shear strength parameters of intact rock

Kamil KAYABALI[a*] and Atakan BALCI[b]

[a] *Department of Geological Engineering, Ankara University, 06830, Ankara, Türkiye.*
[b] *Department of International Affairs, The General Directorate of Ilbank, 06560, Ankara, Türkiye.*

Research Article

Keywords:
Intact Rock, Shear Strength Parameters, Triaxial Compression Test, Uniaxial Compression Test, Single-Shear Test.

Received Date: 23.12.2024
Accepted Date: 05.01.2026

ABSTRACT

Engineering structures built on or within rock masses require a proper characterization of their geomechanical properties. In this context, determining the strength parameters of intact rock is essential. Triaxial compression (3XC) tests are routinely employed to determine the cohesion (c) and friction angle (ϕ) of intact rocks. However, this test not only involves inherent uncertainties but also typically requires a full day to complete a single set of samples. The objective of this study is to evaluate a more practical approach for determining the c and ϕ of intact rocks. For this purpose, 20 types of intact rock were tested via 3XC, uniaxial compression (UC), and single-shear (SS) methods. The internal friction angles were determined from UC tests, while the cohesion values were obtained from SS tests. The c-ϕ pairs derived from the 3XC tests were compared with those obtained from the UC and SS tests. The results indicate that SS tests tend to overestimate cohesion compared to 3XC tests, whereas UC tests generally underestimate friction angles. Overall, the findings suggest that the proposed approach has potential as an alternative testing method in rock mechanics.

1. Introduction

Civil engineering structures such as highways, railways, tunnels, ports, open-pit excavations, and slopes are constructed on or within soils and rock masses. For geotechnical projects built on or within rock masses, the geomechanical properties of the rock mass must be characterized accurately (Diamantis et al., 2016). The shear strength of a rock mass is controlled primarily by two components: intact rock and discontinuity planes. Determining each component requires different experimental techniques. This investigation focuses on the intact-rock component.

Determination of the shear-strength parameters of intact rocks is most commonly carried out using direct shear (DS) or 3XC tests (American Society for Testing and Materials 2016 for the direct shear test and ISRM 2007 for the triaxial compression test) (Li et al., 1999; Ramamurthy, 2001; Jiang et al., 2004; Barla et al., 2010; Jia and Shi, 2011; Gong et al., 2019). However, each testing method has inherent difficulties and/or disadvantages in terms of practicality. For instance, Kömürlü and Demir (2018) discussed the disadvantages of the DS test on intact rocks -particularly for high-strength specimens- as: i) possible failure of the cement mortar instead of the rock-core specimens; ii) impractical specimen-preparation procedures, including two-step cement-mortar casting; iii) the need to wait several days for curing of the cast mortar; iv) significant bending/tension effects on the rock specimen when loaded in the soft cement mortar, leading to lower strength

Citation Info: Kayabalı, K., Balcı, A. 2026. An Alternative approach to estimate the shear strength parameters of intact rock. Bulletin of the Mineral Research and Exploration 179, 124-137. https://doi.org/10.19111/bulletinofmre.1856342

Corresponding author: Kamil KAYABALI, kayabali@ankara.edu.tr

values than those under pure-shear conditions; and v) problems related to adjustment of the gap dimension between the two-step cast mortars. Despite its relative simplicity compared to DS, 3XC testing is time-consuming, costly, and requires a large number of well-prepared (regularly shaped) specimens and appropriate testing procedures (Diamantis et al., 2016). This technique is destructive, and samples of the required quality are difficult to obtain, especially from highly jointed and friable rocks (Shahani et al., 2022). In addition, placing and removing specimens in the Hoek cell also complicates the experiment (Karaman et al., 2013).

The uniaxial compressive strength (UCS), which represents the combined effect of the two strength parameters -cohesion and internal friction angle- as a single value, is probably the most commonly used index parameter for quantifying the strength of intact rocks. Consequently, the uniaxial compression (UC) test is the most frequently employed testing method in rock mechanics and rock engineering. Similar to the DS and 3XC tests, there are standardized procedures for conducting the UC test (ASTM D2398; American Society for Testing and Materials, 2002*a*). However, the UC test is also laborious and time-consuming. For these reasons, considerable efforts have been devoted to developing fast and cost-effective indirect estimators of UCS, such as the point-load test (Broch and Franklin, 1972), Schmidt hammer test (ASTM C805; American Society for Testing and Materials, 2002*b*), sound velocity test (ASTM C597; American Society for Testing and Materials, 2002*c*), impact strength test (Fener et al., 2005), Los Angeles abrasion test (Shakoor and Brown, 1996; Shahani et al., 2022), and nail penetration test (Kayabalı and Selçuk, 2010; Selçuk et al., 2012; Palassi and Emami, 2014).

In the design and numerical modeling of underground openings, excavations, and foundations in rock, the Mohr -Coulomb shear-strength parameters-cohesion (c) and friction angle (ϕ)—are frequently required (Sivakugan et al., 2014). These parameters are also commonly used to assess the damaged zones in rock masses surrounding excavations and to design appropriate support systems (Srivastava and Singh, 2015; Wu et al., 2018). Alidaryan et al. (2023) reported that an increase in the depth of underground excavations leads to a greater contribution of the intact rock to the failure process than that of rock discontinuities. Therefore, investigating the variation of the strength components of intact rock materials is essential for the stability analysis of deep underground openings.

Owing to the high cost and time requirements, 3XC tests are often unavailable at the early stages of a project; thus, designers must estimate rock strength in the absence of 3XC data (Cai, 2010). Several researchers have examined the applicability of the UC test and uniaxial tensile strength (UTS) in estimating c and ϕ when 3XC data are not available (Shahani et al., 2022). For instance, Karaman et al. (2015) employed the Brazilian test (BT) to estimate UCS and the shear-strength parameters of rocks, concluding that BT values can be used to estimate UCS and cohesion. However, no consistent relationship was observed between the internal-friction angle and either UCS or BT for all tested rock types.

Kalantari et al. (2018) developed a method based on the limit-equilibrium-of-forces model to estimate cohesion, internal-friction angle, and UCS for three rock types -weak, medium, and high-strength- using operational drilling data. Their findings indicated that the estimated parameters derived from drilling data were in good agreement with those obtained from conventional laboratory experiments. Similarly, Sivakugan et al. (2014) proposed a theoretical approach to determine these two parameters from UC and indirect tensile strength tests. Their results showed that the predicted cohesion values were generally more reliable than the friction-angle values, and the observed scatter was attributed to anisotropy and heterogeneity within the rock cores.

Kömürlü and Demir (2018) employed a double-shear jaw (DSJ) apparatus to assess whether it can be effectively used to evaluate the cohesion of intact rocks. They conducted a series of numerical analyses to compare the DSJ results with those obtained from experimental studies and to investigate the stress distribution within the core specimens loaded by the DSJ, aiming to determine the ideal failure shape and jaw dimensions. They concluded that, rather than shearinduced failures, tensile failures were predominantly observed under conventional shear testing conditions. Accordingly, they proposed a modified DSJ design to ensure valid failures governed by shear stresses during cohesion determination.

Karaman et al. (2013) conducted Brazilian, UC, and 3XC tests on 37 different rock samples to indirectly determine the cohesion and internal friction angle of intact rocks. They performed a series of regression analyses and found that cohesion could be reliably estimated using indirect tensile (i.e., Brazilian) and UC tests without the need to perform 3XC tests (r = 0.94). However, a meaningful relationship between the estimated and measured ϕ values could not be established.

Recent studies have also applied intelligent approaches to estimate the cohesion (c) and internal friction angle (ϕ) of rocks using indirect methods. Shahani et al. (2022) employed four advanced machine-learning-based predictive models. Their results indicated that the support vector machine (SVM) was the most efficient model for predicting c ($R^2 = 0.98$) and ϕ ($R^2 = 0.92$), with UCS and tensile strength identified as the most influential parameters. Shen and Jimenez (2018) used genetic programming (GP) to develop a predictive model for estimating the Mohr-Coulomb shear-strength parameters of intact sandstone from other strength measures (UCS and UTS) under stress conditions leading to shear failure. They evaluated the reliability of the GP model and compared it with linear regression models based solely on UCS or UTS, as well as with the conventional triaxial-based approach. Their results showed that although the triaxial method provides more accurate estimations, the proposed GP model exhibits superior predictive performance in the absence of triaxial data, making it suitable for practical strength estimation of intact sandstone at early project stages or when triaxial test data are unavailable. Shahani et al. (2022) also provided a comprehensive summary of intelligent methods for indirectly determining shear-strength parameters using common index properties of intact rock.

The Mohr-Coulomb (M-C) criterion is one of the most widely used failure criteria for rock. It defines a linear relationship between the shear strength and the normal stress acting on the failure plane at failure and is characterized by two material parameters: cohesion and friction angle (Lee and Bobet, 2014). Although the strength envelopes of intact rock are actually non-linear functions of stress level (Hoek and Brown, 1997), the linear M-C model is still widely employed in practical applications due to its simplicity, mathematical convenience, and its long-standing use in the field (Jimenez et al., 2008; Labuz and Zang, 2012).

The aim of this investigation is to estimate the cohesion and internal friction angle of intact rocks using single-shear (SS) and uniaxial compression (UC) tests. The shear-strength parameters obtained from these two tests are then compared with those determined from triaxial compression (3XC) tests.

2. Materials and Methods

The rock samples used in this study were obtained from commercial companies operating stone quarries in Ankara (Türkiye) and neighboring cities. The majority of the samples were magmatic (both intrusive and extrusive), while sedimentary and metamorphic rocks were also included to cover a broader range of lithologies. The petrographic properties of these rocks, including mineralogical composition and texture type, are summarized in Table 1. The samples were initially in the form of cubic blocks with 15-cm sides. Core specimens of 54 mm in diameter (NX size) were extracted from the blocks according to the standard ASTM D4543 (American Society for Testing Materials, 2001). The edges of the specimens were cut parallel and smooth, and the length-to-diameter ratio (L/D) was maintained between 2 and 2.5. The test specimens had proper cylindrical shapes with smooth sides and were free from abrupt irregularities. Special care was taken to ensure that the samples exhibited no visible anisotropy. For the planned mechanical tests, 10 core specimens were initially prepared for each rock type (Figure 1).

Five uniaxial compression (UC) tests were conducted on core specimens according to the ASTM D2938 standard (American Society for Testing and Materials, 2002*a*). Two hydraulic presses with

Table 1- Types of rocks used in the investigation and their petrographical properties.

No.	Texture	Mineralogical composition	Rock name
01	Hyalopilitic-porphyritic (zoning, glomera porphyritic)	Plagioclase, amphibole, biotite, crystallite, microlite	Andesite
02	Holocrystalline porphyritic (zoning)	Plagioclase, pyroxene, amphibole	Diorite porphyr
03	Sparitic	Mainly calcite, occasionally recrystallized calcite	Limestone
04	Hyalo-clastic (corrosion)	Quartz, plagioclase, andesite fragments, volcanic glass splinters, amphibole, opaque minerals, pumice fragments	Tuff (vitric)
05	Sparitic	Mainly sparite, calcite, fossil and shells	Fossiliferous limestone, biosparitic limestone
06	Micritic	Mainly calcite, opaque minerals	Limestone (traverine-limestone contact)
07	Granoblastic (polygonal)	Mainly calcite	Marble
08	Micritic	Mainly calcite and recrsytallized calcite	Recrystallized limestone
09	Sparitic, crystallized	Mainly calcite	Recrystallized limestone
10	Crystallene	Abundance of calcite	Crystalline limestone
11	Sparitic	Mainly calcite, fossils, and shell fragments	Fossiliferous limestone
12	-	Mainly calcite and recrsytallized calcite	Travertine
13	Granoblastic (polygonal)	Mainly calcite	Marble
14	Kidney-like	Mainly calcite	Cold-water travertine
15	Micritic	Mainly calcite	Micritic limestone
16	Hyalopilitic- porphyritic (flow, zoning, glomera porphyritic)	Biotite, pyroxene, amphibole, matrix (crystallite, microlite), plagioclase, opaque minerals	Andesite (basaltic andesite)
17	Hyalino-clastic (zoning)	Basalt fragments, plagioclase, biotite, volcanic glass splinters, opaque minerals, dacitic rock fragments	Ignimbrite
18	Hypo-hyaline (vesicular)	Crystallite, microlite, volcanic glass, pyroxene	Basalt
19	Hyalino-clastic (zoning)	Plagioclase, quartz, biotite crystals, dacitic fragments, zeolite, pumice fragments	Zeolitized tuff
20	Hyalino-clastic (zoning, corrosion)	Plagioclase, quartz, basaltic rock fragments	Ignimbrite

Figure 1- Views of core specimens prepared for mechanical tests.

capacities of 200 kN and 1000 kN were used to perform the UC tests. The higher-capacity press was employed for high-strength rock samples, whereas the lower-capacity press was used for low-strength samples. For all tests, the ends of the specimens were cut parallel to each other and perpendicular to the longitudinal axis. The spherical seat was checked to ensure it could rotate freely in its socket before each test. Two steel platens were used to transmit the axial load to the specimen ends. The loading rates were selected so that specimen failure occurred within 2-15 minutes.

Triaxial compression (3XC) tests on the rock samples were conducted following the guidelines of ASTM D2664 (American Society for Testing and Materials, 1995). Similar to the UC tests, the loading rate was controlled so that specimen failure occurred within 2-15 minutes. After each test, the specimen membrane was carefully inspected for fissures or punctures to ensure that no testing fluid had penetrated the specimen. Three 3XC tests were performed for each rock sample, using confining pressures of either 0.5-1.0-1.5 MPa or 1.0-2.0-3.0 MPa, depending on the UCS of the sample. The lower set of pressures was used for low-strength rocks, while the higher set was applied to high-strength specimens. Occasionally, inconsistencies in the Mohr circles were observed, preventing the construction of a valid Mohr envelope. Such results were most likely caused by inhomogeneities or anisotropies not detectable macroscopically. In these cases, the full set of 3XC tests was repeated to ensure the construction of a meaningful Mohr envelope.

As discussed earlier, performing 3XC tests on rocks is cumbersome. One of the main difficulties is the removal of hydraulic oil when the specimen membrane is damaged. While some advanced testing machines can withdraw the confining fluid automatically, this step must be performed manually with most conventional 3XC machines, making the process messy and laborious. Conducting a full set of 3XC tests using conventional equipment may take up to a full day in some cases. To estimate the shear-strength parameters of intact rocks more practically, the ring-shear (RS) test method was selected as an alternative technique. The hypothesis of this study is that if the cohesion (y-intercept) obtained from a ring-shear test, combined with the Mohr circle from a UC test, can produce a Mohr envelope closely matching that from the 3XC test for the same rock specimens, then the cohesion and internal friction angle of intact rocks can be determined in a much more practical manner.

The ring-shear (RS) test (Figure 2), originally proposed by Lundborg (1966), provides a relatively simple method for evaluating the shear strength of intact rocks as a function of confining pressure (Goodman, 1991). When the confining pressure is zero, the cohesion is calculated as $c = P/2A$, where P is the load at failure and A is the cross-sectional area of the cylindrical core specimen. To address the first part of the hypothesis, the test setup -a modified version of the apparatus devised by Lundborg (1966) and shown in Figure 3- was manufactured.

3. Experimental Results

Triaxial compression tests on the rock specimens were intentionally conducted at low confining pressures for two reasons. First, when rock materials are tested at high stress levels, a non-linear response may occur, which increases the cohesion intercept while decreasing the friction angle

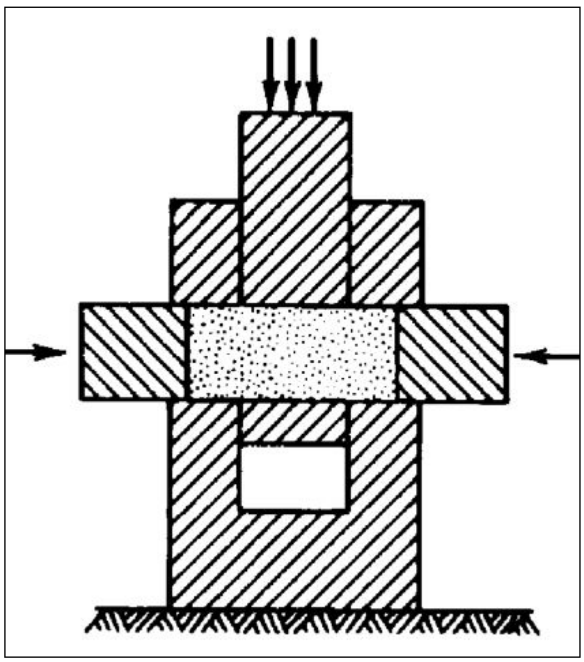

Figure 2- Ring shear device developed by Lundborg (1966).

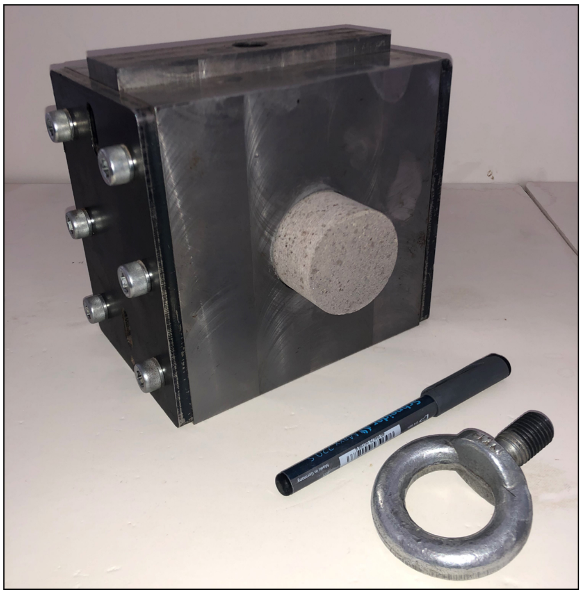

Figure 3- Modified ring shear apparatus employed for this investigation.

(Ramamurthy, 2001). Second, the capacity of the triaxial press used was limited. Three specimens from each rock sample were subjected to different confining pressures, and the deviatoric stresses at failure were recorded. A representative plot of axial stress versus axial strain for rock sample No. 10 is presented in Figure 4. Other similar graphs are not shown to save space. Only the Mohr diagrams are included, as shown in Figure 5(i-u). The Mohr envelope for each sample was constructed analytically in Excel. The points tangent to the last two Mohr semicircles were determined, and a straight line passing through these points was drawn, extending the ordinate. Cohesion and internal friction angle values were then calculated and are listed in Table 2 for the 20 rock samples.

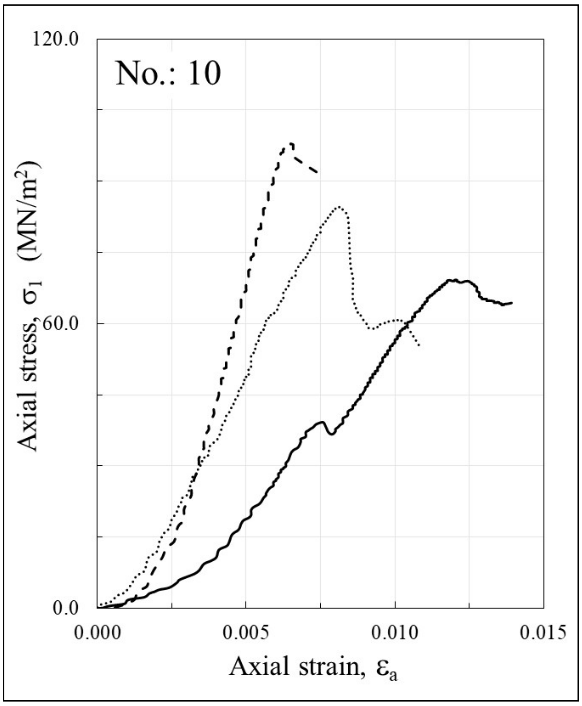

Figure 4- An example plot of axial stress versus axial strain obtained from triaxial compression tests.

Table 2- Results of triaxial tests.

No.	c (MPa)	ϕ (º)
01	11.7	54.9
02	5.6	66.4
03	8.4	54.9
04	5.5	51.1
05	2.7	48.6
06	7.0	65.9
07	17.8	45.6
08	7.3	63.5
09	8.2	68.6
10	3.4	70
11	9.3	71.1
12	8.0	72.5
13	8.2	65.4
14	18.3	61
15	9.0	67.4
16	5.1	70
17	14.2	25.4
18	14.3	30
19	5.4	54.9
20	3.0	48

For the UC tests, five specimens from each rock sample were tested to determine the uniaxial compressive strength (UCS). A representative plot of the UC test for sample No. 10 is presented in Figure 6. Results for the other 19 rock samples are not shown graphically to save space; instead, they are summarized in Table 3 as minimum, maximum, and mean values.

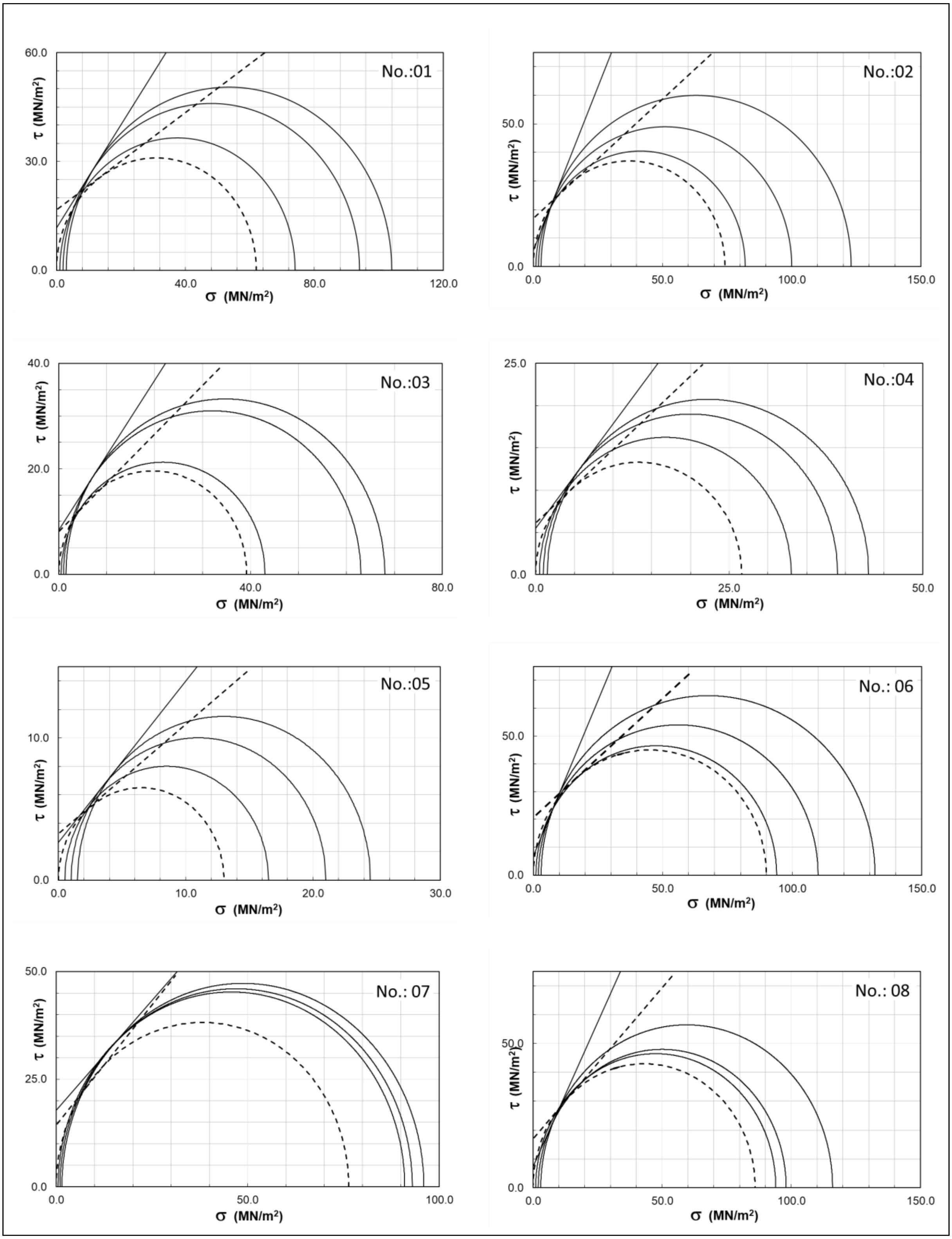

Figure 5- Mohr diagrams of 20 different rock samples tested. The dashed circles and envelopes represent 1XC tests.

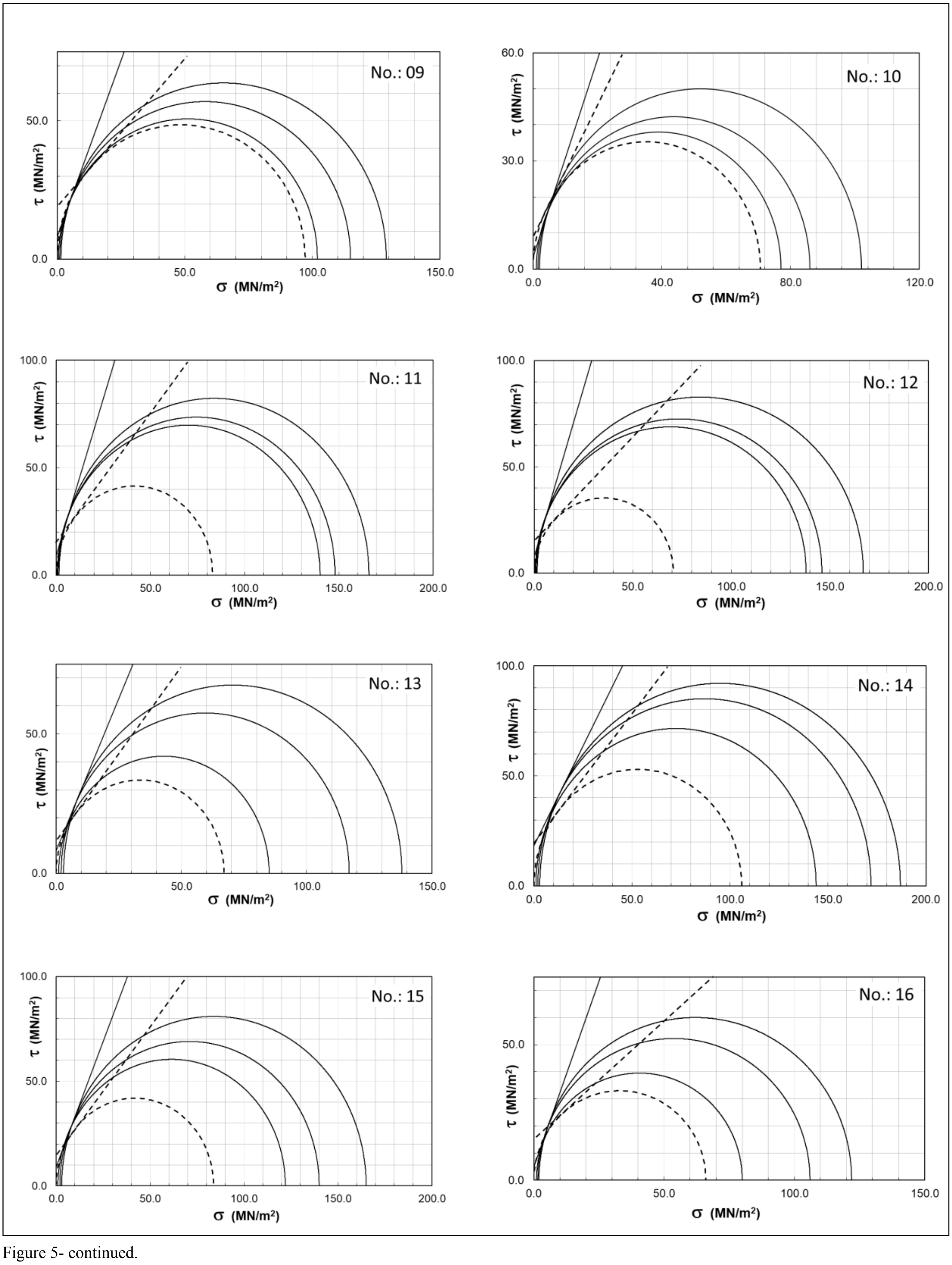

Figure 5- continued.

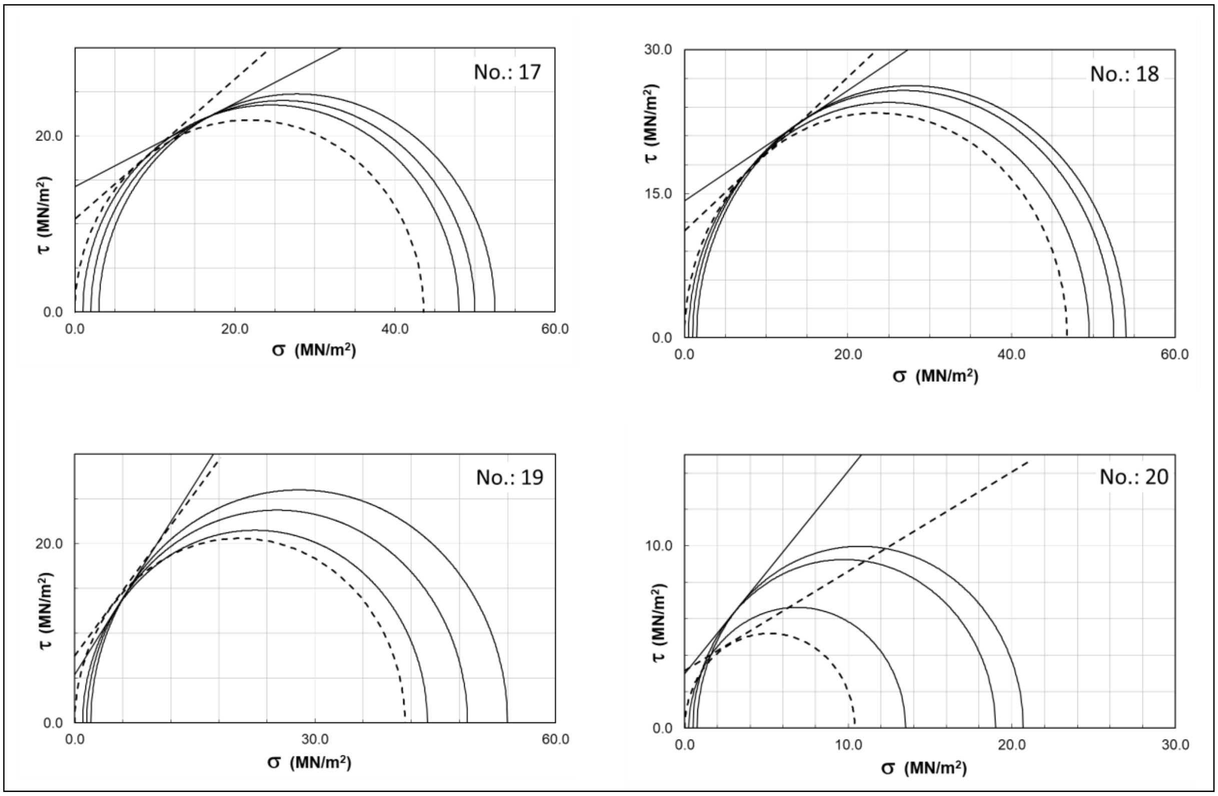

Figure 5- continued.

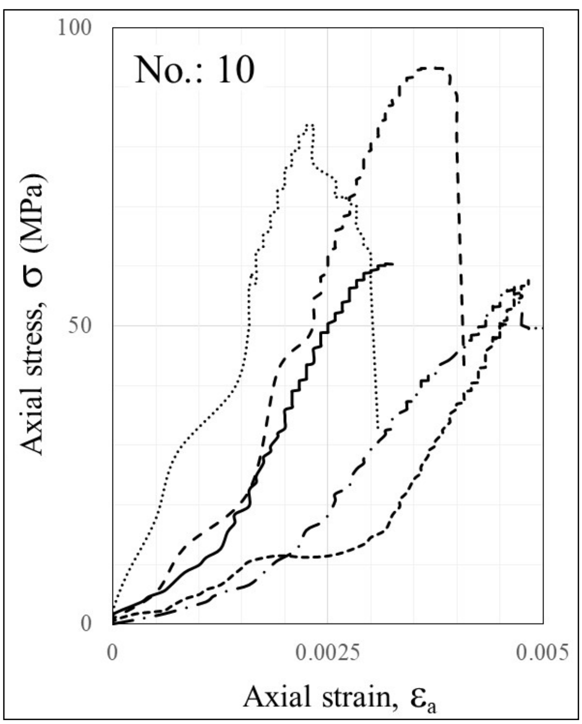

Figure 6- An example plot of axial stress versus axial strain obtained from uniaxial compression tests.

Table 3- UCSs for 20 types of rocks (in MPa).

No.	Min.	Max	Mean
01	49	73	62.0
02	68	83	74.2
03	30	50	39.2
04	24	29	26.6
05	8.8	18.5	13.1
06	68	113	90.4
07	61	89	76.4
08	61	99	86.0
09	62	121	97.2
10	57	93	70.6
11	63	101	83.0
12	40	98	70.6
13	48	87	67.0
14	80	128	106
15	64	95	83.8
16	45	82	66.0
17	38	47	43.6
18	39	54	46.8
19	35	48	41.2
20	8.8	12	10.4

For the determination of cohesion of intact rocks, the setup shown in Figure 3 was employed. Initially, a rock core of 54 mm diameter and 120 mm length was fully inserted into the circular slot of the double ring-shear apparatus. In almost all early tests, the failed specimens exhibited sub-vertical failure planes, which was identified as a flexural type of failure due to the three components of the double-shear setup not being held together rigidly. To address this, two vertical plates, as shown in Figure 3, were firmly attached parallel to the longitudinal axis of the circular slot, while the middle part of the apparatus was left free to move during loading. A 0.3 mm gap between the middle component and the outer components was maintained to prevent flexural bending and to minimize friction development between the apparatus components during loading.

Once the rigidity of the apparatus was ensured, the preserved rock cores were subjected to shear tests, which were repeated three times on several rock samples. Early trials revealed two main issues. First, the two shear planes did not always develop simultaneously; one part of the core failed before the other, producing cohesion values that were not comparable to those from the 3XC tests. This was likely due to the uneven distribution of microcracks in the specimens. Second, when both shear planes failed simultaneously, the resulting cohesion was often several times higher than that obtained from the 3XC tests. Consequently, an alternative approach was adopted: all subsequent cohesion tests were conducted along a single shear plane only.

Depending on core availability, five to eight single-shear tests were performed for each rock sample. Figure 7 illustrates the comparison between the cohesions obtained from the double-shear and single-shear tests for rock sample No. 10. The minimum, maximum, and average cohesion values for each rock type obtained from the single-shear tests are presented in Table 4. As shown, cohesions from single-shear tests ranged from 3.4 to 21.9 MPa, whereas the corresponding 3XC test results ranged from 0.8 to 18.3 MPa.

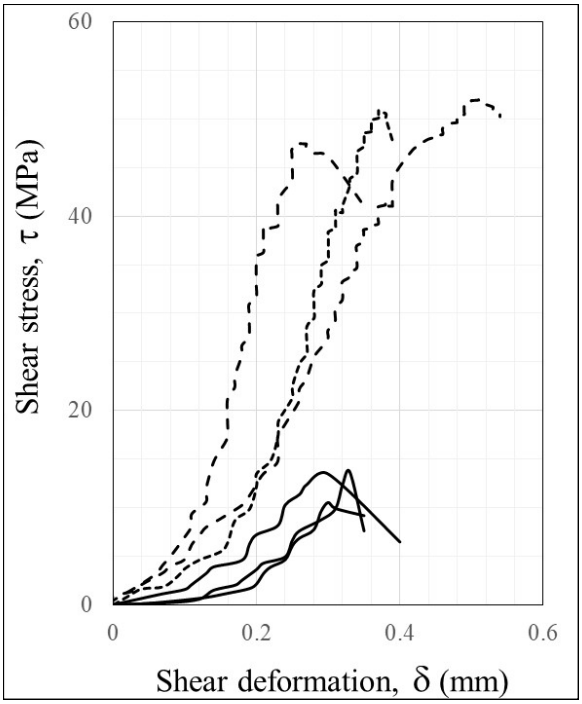

Figure 7- Plot of double- and single-shear tests run on sample No. 10 (dashed lines represent the double-shear test results and solid lines are for single-shear tests).

Table 4- Cohesions obtained from single shear tests (in MPa).

No.	Min.	Max	Mean
01	14.4	19.0	16.6
02	13.2	20.7	15.9
03	6.6	11.0	8.8
04	3.9	8.3	5.7
05	2.7	3.5	3.1
06	14.1	28.3	21.9
07	10.7	17.2	14.7
08	10.4	24.4	18.0
09	14.8	23.6	18.0
10	9.1	13.7	11.6
11	12.3	19.3	15.9
12	12.0	20.6	16.2
13	9.3	15.9	11.9
14	12.2	26.4	18.7
15	11.7	20.0	14.2
16	14.4	20.3	17.1
17	9.4	13.1	11.2
18	7.0	14.7	11.6
19	6.7	8.0	7.5
20	3.2	4.1	3.4

After determining the cohesion values from the single-shear tests, the internal friction angles were calculated analytically using the UC test data (Figure 8). For this purpose, the angular relationships, together with the cohesion intercept and the center of the Mohr circle, were used to calculate the internal friction angle.

To compare the shear-strength parameters obtained from the 3XC tests with those derived from the combination of single-shear and UC tests, Table 5 was prepared. A brief inspection of Table 5 indicates that the cohesion values determined from the single-shear tests are systematically higher than those obtained from the 3XC tests. In contrast, the internal friction angles calculated using the single-shear and UC tests are systematically lower than those from the 3XC tests.

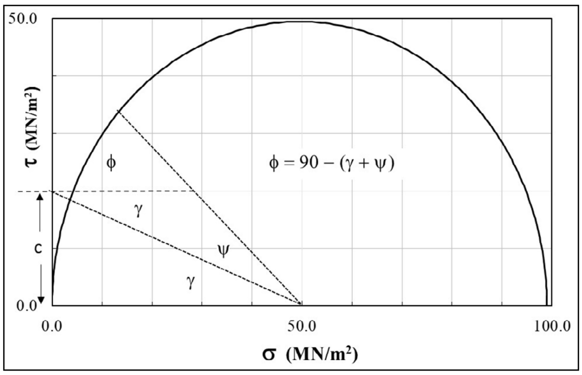

Figure 8- Plot showing the calculation of internal friction angle on a Mohr circle of a 1XC test along with the cohesion from the single-shear test.

Table 5- Shear strength data obtained from triaxial tests and from the proposed method.

No.	From triaxial		From hypothesis	
	c (MPa)	ϕ (°)	c (MPa)	ϕ (°)
01	11.7	54.9	16.5	34.0
02	5.6	66.4	15.8	43.9
03	8.4	54.9	8.8	41.6
04	5.5	51.1	5.7	43.6
05	2.7	48.6	3.2	37.6
06	7.0	65.9	21.8	38.3
07	17.8	45.6	14.7	47.9
08	7.3	63.5	17.9	44.8
09	8.2	68.6	18	49.4
10	3.4	70	11.6	53.6
11	9.3	71.1	15.9	48.1
12	8.0	72.5	16.2	40.7
13	8.2	65.4	11.9	50.9
14	18.3	61	18.7	53.1
15	9.0	67.4	14.2	52.6
16	5.1	70	17.1	35.2
17	14.2	25.4	11.2	35.6
18	14.3	30	11.6	37.3
19	5.4	54.9	7.5	50.0
20	3.0	48	3.4	23.6

Although this trend can be readily inferred from Table 5, a comparative illustration of the two shear-strength parameters obtained from the different methods is presented in Figure 9. In Figure 9, circles represent the c-ϕ pairs from the 3XC tests, whereas squares represent the c-ϕ pairs from the single-shear and UC tests. Approximately two-thirds of the data indicate a systematic increase in cohesion accompanied by a systematic decrease in internal friction angles. Several data pairs (e.g., Nos. 3, 4, 5, 14, 20) show a marked drop in friction angle while cohesion remains nearly constant. Three other data sets (Nos. 7, 17, 18) exhibit an increase in friction angles accompanied by a decrease in cohesion. Overall, these observations suggest that the decrease in internal friction angle is largely compensated by an increase in cohesion.

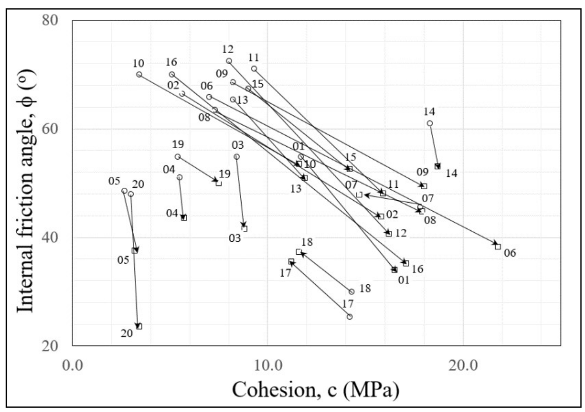

Figure 9- Graph illustrating the comparative relationship between the ϕ pairs of the conventional method and the proposed approach.

In the final phase of the investigation, a comparison was made between the c-ϕ pairs obtained from the 3XC tests and those obtained using the proposed approach, employing the Mohr-Coulomb criterion. An example of this comparison is shown in Figure 10, where the alternative approach overestimates the shear strength (τ) for normal stresses (σ) below approximately 10 MPa.

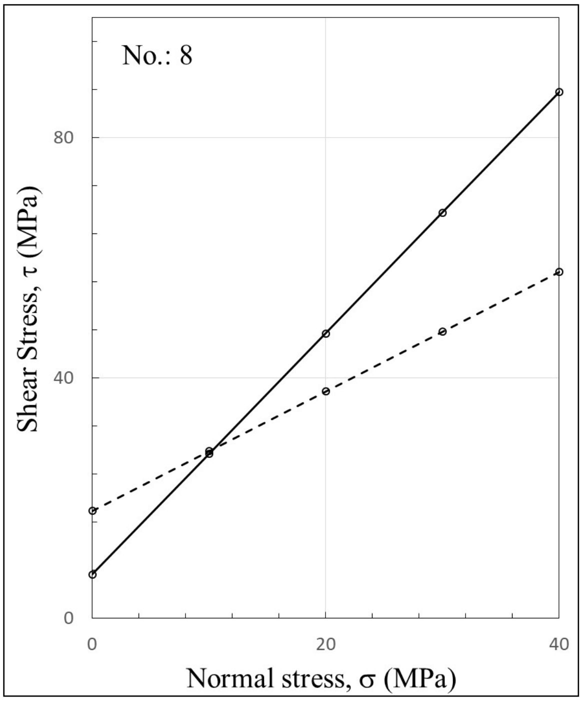

Figure 10- Example plot of Mohr-Coulomb envelopes. The solid line represents the conventional 3X tests, whereas the dashed line is for the proposed approach.

Conversely, the shear strength is underestimated compared to the conventional 3XC data when the normal stress exceeds 10 MPa. This trend generally holds for the other rock types, except for sample No. 7, where the crossover point of the two envelopes occurs at 35 MPa. Overall, the proposed approach produces higher strength values for normal stresses around 10 MPa or less and lower strength values for normal stresses above 10 MPa. This discrepancy is likely due to fundamental differences in the testing and failure mechanisms between the conventional and proposed methods. Accordingly, if the proposed approach is considered a valid method for determining shear-strength parameters, it can be inferred that confining pressure in the conventional 3XC tests increases the internal friction angle while decreasing the cohesion of intact rocks.

To improve the quality of the results, additional statistical relationships between the parameters considered in this study were investigated. The most significant correlation ($R^2 = 0.93$) was found between the cohesion from the single-shear test and the UCS. However, no meaningful statistical relationship could be established between the UCS values obtained in this study and the internal friction angles derived from them. Consequently, regression analyses aimed at identifying empirical relationships between cohesion, internal friction angle, and UCS using the conventional method did not yield any significant results. This outcome can be regarded as an advantage of the proposed alternative method over the conventional approach. Furthermore, considering that UCS can be reliably estimated using practical indirect methods (e.g., Kayabalı and Selçuk, 2010; Selçuk et al., 2012), it can be concluded that the strength parameters of intact rocks can be determined in a highly practical and efficient manner using the proposed method.

4. Conclusions and Discussion

Considering that triaxial compression (3XC) tests, which are commonly used to determine the strength parameters of intact rocks, involve certain inherent uncertainties and are relatively difficult to perform, a hypothesis was proposed in which these parameters could be obtained in a more practical manner. The following concrete results were derived from this study:

In double-shear ring tests, shear failures along the two planes do not always develop simultaneously due to the non-uniform distribution of microcracks and possible inhomogeneities within the core specimens. Cohesion values obtained from experiments where shear failure occurs simultaneously on both planes are substantially higher than those obtained from triaxial compression (3XC) tests.

Although a strong correlation exists between the cohesion values obtained from single-shear tests and those from triaxial compression (3XC) tests, the cohesion values from the former are still 50-80% higher than those from the latter.

The internal friction angles calculated using the cohesion from the single-shear tests in combination with the Mohr circle from the uniaxial compression (UC) tests are generally lower than those obtained from triaxial compression (3XC) tests.

Two types of Mohr-Coulomb failure envelopes were generated using the c-ϕ pairs from the triaxial compression (3XC) tests and those from the proposed method. A comparison of these envelopes shows that, at low normal stresses (σ below approximately 10 MPa), the shear strengths predicted by the proposed method are slightly higher than those from the conventional 3XC tests. Beyond this threshold, the trend reverses: for normal stresses above approximately 10 MPa, the shear strengths calculated using the proposed method are lower than those determined by the conventional method.

The approximate normal stress value of 10 MPa observed in most of the comparative Mohr-Coulomb failure envelopes in this study corresponds to field depths typically less than 400 m. For designs at depths shallower than this, it is recommended that the cohesion obtained using the proposed method be reduced by half. For normal stresses exceeding this threshold, using the cohesion and internal friction angle values directly from the proposed approach will provide conservative and safe estimates for design purposes.

Regression analyses performed on the parameters considered in this study indicated that the strongest empirical relationship exists between the UCS and the cohesion values from single-shear tests. The lack of a comparable relationship for the conventional method suggests that the proposed method may offer certain advantages over the conventional approach.

Considering that UCS can be reliably and practically estimated through indirect methods, it can be concluded that the proposed approach may serve as a valuable alternative for determining the strength parameters of intact rocks.

References

Alidaryan, M., Khosravi, M. H, Bahaaddini, M., Moosavi, M., Roshan, H. 2023. Mobilization of Cohesion and Friction Angle of Intact Rocks in the Shearing Process. Rock Mechanics and Rock Engineering, 1-13.

American Society for Testing Materials. 1995. Standard Test Method for Triaxial Compressive Strength of Undrained Rock Core Specimens Without Pore Pressure Measurements, D2664, 100 Barr Harbor Dr., West Conshohocken, PA, USA.

American Society for Testing Materials. 2001. Standard Practices for Preparing Rock Core Specimens and Determining Dimensional and Shape Tolerances, D4543, 100 Barr Harbor Dr., West Conshohocken, PA, USA.

American Society for Testing Materials. 2002*a*. ASTM D2938, Standard Test Method for Unconfined Compressive Strength of Intact Rock Core Specimens, 100 Barr Harbor Dr., West Conshohocken, PA, USA.

American Society for Testing Materials. 2002*b*. ASTM C805, Standard Test Method for Rebound Number of Hardened Concrete, 100 Barr Harbor Dr., West Conshohocken, PA, USA.

American Society for Testing Materials. 2002*c*. ASTM C597, Standard Test Method for Ultrasonic Pulse Velocity Through Concrete, 100 Barr Harbor Dr., West Conshohocken, PA, USA.

American Society for Testing Materials. 2016. ASTM D5607, Standard Test Method for Performing Laboratory Direct Shear Strength Tests of Rock Specimens Under Constant Normal Force, 100 Barr Harbor Dr., West Conshohocken, PA, USA.

Barla, G., Barla, M, Martinotti, M. E. 2010. Development of a New Direct Shear Testing Apparatus. Rock Mechanics and Rock Engineering 431, 117-122.

Broch, E., Franklin, J. A. 1972. The Point-load Strength Index. International Journal of Rock Mechanics and Mining Sciences 96, 669-697.

Cai, M. 2010. Practical estimates of tensile strength and Hoek-Brown parameter m_i of brittle rocks. Rock Mechanics and Rock Engineering 432, 167-184.

Diamantis, K., Exarhakos, G., Migiros, G., Gartzos, E. 2016. Evaluating the Triaxial Characteristics of Ultramafic Rocks from Central Greece Using the Physical, Dynamic and Mechanical Properties. Open Access Library Journal 312, 1-20.

Fener, M., Kahraman, S., Bilgili, A., Günaydın, O. 2005. A Comparative Evaluation of Indirect Methods to Estimate the Compressive Strength of Rocks. Rock Mechanics and Rock Engineering 38, 329-343.

Goodman, R. E. 1991. Introduction to Rock Mechanics, John Wiley and Sons, 562.

Gong, F. Q., Si, X. F., Li, X. B., Wang, S. Y. 2019. Dynamic Triaxial Compression Tests on Sandstone at High Strain Rates and Low Confining Pressures with Split Hopkinson Pressure Bar. International Journal of Rock Mechanics and Mining Sciences 113, 211-219.

Hoek, E., Brown, E. T. 1997. Practical estimates of rock mass strength. International Journal of Rock Mechanics and Mining Sciences 348, 1165-1186.

ISRM. 2007. The Complete ISRM Suggested Methods for Rock Characterization, Testing, and Monitoring: 1974-2006. Suggested Methods Prepared by the Commission on Testing Methods, International Society for Rock Mechanics, Compilation Arranged by the ISRM Turkish National Group Ankara, Turkey, 628.

Jia, Z. R., Shi, J. 2011. A Method of Data Processing for Determining Shear Strength Parameters of Rock. Applied Mechanics and Materials 97, 397-401.

Jiang, Y., Xiao, J., Tanabashi, Y., Mizokami, T. 2004. Development of an Automated Servo-Controlled Direct Shear Apparatus Applying a Constant Normal Stiffness Condition. International Journal of Rock Mechanics and Mining Sciences 41, 275-286.

Jimenez, R., Serrano, A., Olalla, C. 2008. Linearization of the Hoek and Brown Rock Failure Criterion for Tunnelling in Elasto-plastic Rock Masses. International Journal of Rock Mechanics and Mining Sciences 457, 1153-1163.

Kalantari, S., Hashemolhosseini, H., Baghbanan, A. 2018. Estimating Rock Strength Parameters using Drilling Data. International Journal of Rock Mechanics and Mining Sciences 104, 45-52.

Karaman, K., Cihangir, F., Ercikdi, B., Kesimal, A. 2013. Evaluation of Cohesion and Friction Angle of Intact Rock using Indirect Methods. Mehmet Akif Ersoy Üniversitesi Fen Bilimleri Enstitüsü Dergisi 42, 13-19.

Karaman, K., Cihangir, F., Ercikdi, B., Kesimal, A., Demirel, S. 2015. Utilization of the Brazilian Test for Estimating the Uniaxial Compressive Strength and Shear Strength Parameters. Journal of the Southern African Institute of Mining and Metallurgy 1153, 185-192.

Kayabalı, K., Selçuk, L. 2010. Nail Penetration Test for Determining the Uniaxial Compressive Strength of Rock. International Journal of Rock Mechanics and Mining Sciences 472, 265-271.

Kömürlü, E., Demir, A. D. 2018. Determination of Cohesion Values of Rock Materials using Double Shear Jaws. Periodica Polytechnica. Civil Engineering 624, 881.

Labuz, J. F., Zang, A. 2012. Mohr-Coulomb Failure Criterion. Rock Mechanics and Rock Engineering, 456:975-979.

Lee, Y. K., Bobet, A. 2014. Instantaneous Friction Angle and Cohesion of 2-D and 3-D Hoek-Brown Rock Failure Criteria in Terms of Stress Invariants. Rock Mechanics and Rock Engineering 47, 371-385.

Li, H. B., Zhao, J., Li, T. J. 1999. Triaxial Compression Tests on a Ganite at Different Strain Rates and Confining Pressures. International Journal of Rock Mechanics and Mining Sciences 368, 1057-1063

Lundborg, N. 1966. Triaxial Shear Strength of Some Swedish Rocks and Ores, Proc. 1st Cong. ISRM Lisbon 1, 251-255.

Palassi, M., Emami, V. 2014. A New Nail Penetration Test for Estimation of Rock Strength. International Journal of Rock Mechanics and Mining Sciences 66, 124-127.

Ramamurthy, T. 2001. Shear Strength Response of Some Geological Materials in Triaxial Compression. International Journal of Rock Mechanics and Mining Sciences 385, 683-697

Selcuk, L., Gökce, H. S., Kayabalı, K., Şimşek, O. 2012. A Nondestructive Testing Technique: Nail Penetration Test. ACI Structural Journal 1092, 245-252.

Shahani, N. M., Ullah, B., Shah, K. S., Hassan, F. U., Ali, R.; Elkotb, M. A., Ghoneim, M. E., Tag-Eldin, E. M. 2022. Predicting Angle of Internal Friction and Cohesion of Rocks Based on Machine Learning Algorithms. Mathematics 1020, 3875.

Shakoor, A., Brown, C. 1996. Development of a Quantitative Relationship between Unconfined Compressive Strength and Los Angeles Abrasion Loss for Carbonate Rocks. Bulletin of Engineering Geology & the Environment 531, 97-103.

Shen, J., Jimenez, R. 2018. Predicting the Shear Strength Parameters of Sandstone using Genetic Programming. Bulletin of Engineering Geology and the Environment 77, 1647-1662.

Sivakugan, N., Das, B. M., Lovisa, J., Patra, C. R. 2014. Determination of c and Φ of Rocks from Indirect Tensile Strength and Uniaxial Compression Tests. International Journal of Geotechnical Engineering 81, 59-65.

Srivastava, L. P., Singh, M. 2015. Effect of Fully Grouted Passive Bolts on Joint Shear Strength Parameters in a Blocky Mass. Rock Mechanics and Rock Engineering 483, 1197-1206.

Wu, X., Jiang, Y., Li, B. 2018. Influence of Joint Roughness on the Shear Behavior of Fully Encapsulated Rock Bolt. Rock Mechanics and Rock Engineering 513, 953-959.